

A numerical investigation of a series solution for calculating Z_g of underground power cables

F. A. Uribe, J. L. Naredo, P. Gómez and P. Zúñiga

Abstract-- A numerical investigation of the series solution by Wedepohl *et al.*, for calculating ground-return impedances of underground power cables is presented in this paper. Although this series solution was proposed in 1973, its accuracy, convergence and required processing-time have not been determined. From this investigation, a new hybrid technique is proposed (analytical-numerical) for the practical evaluation of ground-return impedances of underground cables for most engineering application cases.

The results obtained here show that its accuracy is comparable to the direct solution of the Pollaczek's integral, its convergence is uniform as the Wedepohl series solution and its processing-time is short as a closed-form approximation.

Keywords: series solution, ground-return impedances, power cables, electromagnetic transients.

I. INTRODUCTION

IN 1973 Wedepohl *et al.* presented a mathematical model for the analysis of frequency dependent travelling-wave phenomena in underground transmission systems suitable for steady-state or transient analyzes. In this model the wave-propagation characteristics of the system are given by the natural modes where the skin effect in conductors and ground is directly taken into account [1]. An important contribution of this paper is the solution of the Pollaczek's integral through low-frequency infinite series.

In 1926, Pollaczek presented a set of non-analytic integral expressions to calculate the electric field due to an infinite thin filament of current in the presence of an imperfect conducting ground [2].

An initial study of the model solution developed in [1] indicates that combining the rapidly converging series for the low frequency range with the trapezoidal integration of the exponential integral expression for high frequencies can be used to obtain an accurate and rapid ground-return impedance (Z_g) evaluation [3].

However, to the best knowledge of the authors, an efficient solution of Wedepohl *et al.* series has not been implemented or included yet in any EMTP type software. This may be due to

the preferred use of closed-form approximations for many practical engineering applications, which are accurate enough, although up to date their applicability ranges remain unknown [4, 5].

A numerical investigation of the Wedepohl *et al.* series solution for calculating Z_g of buried power cables is performed in this paper. Resulting from a complementary investigation derived from [3] a new revised vector-based version of this series is interpreted and implemented here. The behavior of this series solution is analyzed here to evidence its rapid and uniform convergence at the low-frequency range [6].

From the above results we propose a new Z_g analytical-numerical evaluation technique combining the solution of Bessel functions with the simple numerical integration (*i.e.*, using the trapezoidal rule) of the exponential function expressions that precedes the series expansion solution in [1].

Further, a computational analysis is developed in this paper similar to the one in [7] comparing three different techniques to solve Pollaczek integral regarding accuracy and CPU-time. The first is with the Wedepohl *et al.* series, the second uses the direct numerical integration of Pollaczek integral with infinite limits applying the Gauss-Kronrod routine and the third is with the closed-form approximation proposed by Saad, Gaba & Giroux based in part on the method of images [4].

Finally, the obtained results show that the here proposed methodology can be used for accurate calculation of Z_g of cable systems and also as an aid to validate other methodologies or closed-form approximations.

II. EARTH-RETURN IMPEDANCES

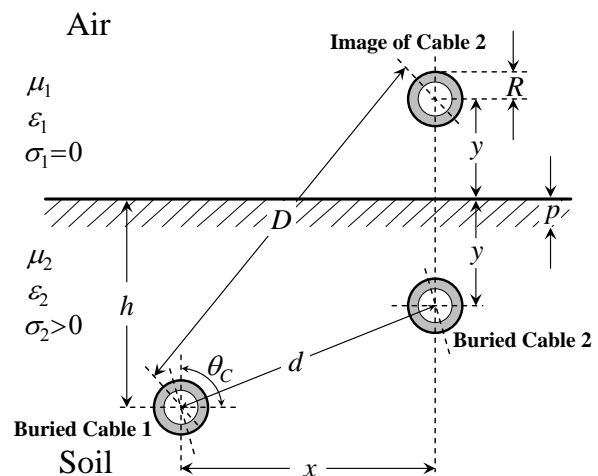


Fig. 1. Geometry of an underground power transmission system

F. A. Uribe and P. Zúñiga are with The State University of Guadalajara, CUCEI, Guadalajara, Jalisco, México (e-mail: felipe.uribe@cucei.udg.mx).
J. L. Naredo is with Cinvestav Guadalajara, Guadalajara, Zapopan, Jal., México.

P. Gómez is with the Department of Electrical and Computer Engineering, Western Michigan University, Kalamazoo, MI, USA.

A. Basic Relations

The self and mutual earth-return impedances for a quasi-TEM_z mode is described by (check Fig. 1 for reference directions) [1]:

$$Z_g(\omega) = \frac{j\omega\mu}{2\pi} \int_{-\infty}^{\infty} \left[\frac{e^{-|y+h|\sqrt{\alpha^2+1/p^2}}}{|\alpha| + \sqrt{\alpha^2+1/p^2}} + \frac{e^{-|y-h|\sqrt{\alpha^2+1/p^2}} - e^{-|y+h|\sqrt{\alpha^2+1/p^2}}}{2\sqrt{\alpha^2+1/p^2}} \right] e^{j\alpha x} d\alpha \quad (1a)$$

where ω represents the angular frequency (in rad/s), μ corresponds to the magnetic permeability (H/m) of the soil, and the complex depth (considering displacement currents) is given by

$$p = 1 / \sqrt{j\omega(\sigma + j\omega\varepsilon_r)\mu} \quad (1b)$$

After the second term of the integral in (1a) is expressed via Bessel functions, (1a) becomes (parameters D and d are shown in Fig.1):

$$Z_g(\omega) = \frac{j\omega\mu}{2\pi} [K_o(D/p) - K_o(d/p) + J_{Poll}] \quad (2)$$

Where:

$$J_{Poll} = (I_2 - 2I_3 + I_4)p^2 \quad (3a)$$

$$I_2 = \int_{-\infty}^{\infty} \sqrt{\alpha^2+1/p^2} \cdot e^{-(h+y)\sqrt{\alpha^2+1/p^2}} e^{j\alpha x} d\alpha \quad (3b)$$

$$I_3 = \int_0^{\infty} \alpha e^{-(h+y)\sqrt{\alpha^2+1/p^2}} e^{j\alpha x} d\alpha \quad (3c)$$

$$I_4 = \int_{-\infty}^{\infty} \alpha e^{-(h+y)\sqrt{\alpha^2+1/p^2}} e^{j\alpha x} d\alpha \quad (3d)$$

According to (3b) and (3d), the solution for I_2 and I_4 is given by:

$$I_2 = \frac{2(h+y)^2}{D^2 p^2} K_2(D/p) + \frac{2[(h+y)^2 - x^2]}{D^3 p} K_1(D/p) \quad (4a)$$

$$I_4 = \frac{2jx(h+y)}{D^2} K_2(D/p) \quad (4b)$$

respectively, where K_1 and K_2 represent modified Bessel functions of first and second order, respectively. For I_3 , we have [1]:

$$I_3 = \frac{1}{D^2 p^2} \int_{(h+y)/D}^{\infty} [(h+y)^2 - x^2] t e^{-Dt/p} dt + \dots \\ \dots + \frac{jx(h+y)}{D^2 p^2} \int_1^{\infty} \left[\frac{1}{\sqrt{t^2-1}} + 2\sqrt{t^2-1} \right] e^{-Dt/p} dt + \dots \\ \dots + \frac{x(h+y)}{D^2 p^2} \int_{(h+y)/D}^1 \left[2\sqrt{1-t^2} - \frac{1}{\sqrt{1-t^2}} \right] e^{-Dt/p} dt \quad (4c)$$

The first component of the integral in (4c) can be easily evaluated by using traditional integration rules; the second part corresponds to $K_2(D/p)$. In [1], it is proposed that the third component of (4c) be evaluated by a series expansion of the exponential function and then be integrated term-by-term to give $S_{ser}(D/p, |x|, \ell)$, with $\ell=h+y$.

This is,

$$I_3 = \frac{[(h+y)^2 - x^2]}{D^4} [1 + (h+y)/p] e^{-(h+y)/p} + \dots \\ \dots + \frac{jx(h+y)}{D^2} K_2(D/p) + \dots \\ \dots + \frac{x(h+y)^2}{D^2 p^2} S_{ser} \left(\frac{D}{p}, |x|, \ell \right) \quad (4d)$$

The series term S_{ser} from (4d) is further analyzed in the following sections.

B. Wedepohl and Wilcox series

Despite a few typographical errors in [1] regarding the converging series, these can be split up into the following four types of terms:

$$S_{ser} \left(\frac{D}{p}, |x|, \ell \right) = S_1 + S_2 + S_3 + S_4 \quad (5)$$

S_1 to S_4 are rearranged into a different form than in [1] and presented in this paper. This is due in part to the fact that the original paper presented typographical errors that can confuse the non-specialist reader. For instance, an analysis of S_1 , given by (6a), reveals that the leading terms:

$$\frac{1}{k(k+2)!} \quad \text{and} \quad \left(\frac{D}{p} \right)^{k+2}, \quad k = 2, 3, \dots$$

can be stored into two separate vectors and used whenever is required. In addition, it can be observed in (6)-(9) the nesting nature of the numerical remaining terms. As an example, a pseudo-code (based on Matlab® programming notation) has been added after the first term (6a). For the second, third, and fourth terms, very similar pseudo-codes (not shown here) can be generated.

First term S_1

$$S_1 = \left\{ \left(\theta - \frac{\ell \cdot |x|}{D^2} \right) + \dots \right. \\ \dots + \frac{1}{2(2!)} \left(\frac{D}{p} \right)^2 \left\{ \frac{\ell \cdot |x|^3}{D^4} + \frac{1}{2} \left(\theta - \frac{\ell \cdot |x|}{D^2} \right) \right\} + \dots \\ \dots + \frac{1}{3(4!)} \left(\frac{D}{p} \right)^4 \left\{ \frac{\ell^3 \cdot |x|^3}{D^6} + \frac{3}{4} \left[\frac{\ell \cdot |x|^3}{D^4} + \frac{1}{2} \left(\theta - \frac{\ell \cdot |x|}{D^2} \right) \right] \right\} + \dots \\ \dots + \frac{1}{4(6!)} \left(\frac{D}{p} \right)^6 \left\{ \frac{\ell^5 \cdot |x|^3}{D^8} + \frac{5}{6} \left[\frac{\ell^3 \cdot |x|^3}{D^6} + \frac{3}{4} \left[\frac{\ell \cdot |x|^3}{D^4} + \frac{1}{2} \left(\theta - \frac{\ell \cdot |x|}{D^2} \right) \right] \right] \right\} + \dots \\ \dots + \frac{1}{5(8!)} \left(\frac{D}{p} \right)^8 \left\{ \frac{\ell^7 \cdot |x|^3}{D^{10}} + \frac{7}{8} \left[\frac{\ell^5 \cdot |x|^3}{D^8} + \frac{5}{6} \left[\frac{\ell^3 \cdot |x|^3}{D^6} + \frac{3}{4} \left[\frac{\ell \cdot |x|^3}{D^4} + \frac{1}{2} \left(\theta - \frac{\ell \cdot |x|}{D^2} \right) \right] \right] \right] \right\} + \dots \right\} \quad (6a)$$

Pseudo-code for S_1

$$\begin{aligned}
 & \text{factor_1} = \theta - \frac{\ell|x|}{D^2}; \\
 & \text{for } k = 1 : N \\
 & \quad \text{factor_1}(k) = \left(\frac{(2k-1)}{2k} * \text{factor_1}(k) + \ell^{(2k-1)} \cdot \frac{|x|^3}{D^{2(k+1)}} \right); \\
 & \quad \text{Coef_1}(k) = \frac{1}{(k+1) \cdot \text{factorial}(2k)} \left(\frac{D}{p} \right)^{2k}; \\
 & \text{end} \\
 & \text{term_1} = (\text{factor_1} * \text{Coef_1}) + \left(\theta - \frac{\ell|x|}{D^2} \right); \tag{6b}
 \end{aligned}$$

Second term S_2

$$\begin{aligned}
 S_2 = & - \left\{ \frac{2}{3(1!)} \left(\frac{D}{p} \right) \left\{ \left(\frac{|x|^3}{D^3} \right) + \dots \right. \right. \\
 & \dots + \frac{2}{5(3!)} \left(\frac{D}{p} \right)^3 \left\{ \frac{\ell^2 \cdot |x|^3}{D^5} + \frac{2}{3} \left(\frac{|x|^3}{D^3} \right) \right\} + \dots \\
 & \dots + \frac{2}{7(5!)} \left(\frac{D}{p} \right)^5 \left\{ \frac{\ell^4 \cdot |x|^3}{D^7} + \frac{4}{5} \left[\frac{\ell^2 \cdot |x|^3}{D^5} + \frac{2}{3} \left(\frac{|x|^3}{D^3} \right) \right] \right\} + \dots \\
 & \dots + \frac{2}{9(7!)} \left(\frac{D}{p} \right)^7 \left\{ \frac{\ell^6 \cdot |x|^3}{D^9} + \frac{6}{7} \left[\frac{\ell^4 \cdot |x|^3}{D^7} + \frac{4}{5} \left[\frac{\ell^2 \cdot |x|^3}{D^5} + \frac{2}{3} \left(\frac{|x|^3}{D^3} \right) \right] \right] \right\} + \dots \\
 & \dots + \frac{2}{11(9!)} \left(\frac{D}{p} \right)^9 \left\{ \frac{\ell^8 \cdot |x|^3}{D^{11}} + \frac{8}{9} \left[\frac{\ell^6 \cdot |x|^3}{D^9} + \frac{6}{7} \left[\frac{\ell^4 \cdot |x|^3}{D^7} + \frac{4}{5} \left[\frac{\ell^2 \cdot |x|^3}{D^5} + \frac{2}{3} \left(\frac{|x|^3}{D^3} \right) \right] \right] \right] \right\} + \dots \tag{7}
 \end{aligned}$$

Third term S_3

$$\begin{aligned}
 S_3 = & - \left\{ \theta + \dots \right. \\
 & \dots + \frac{1}{2(2!)} \left(\frac{D}{p} \right)^2 \left\{ \frac{\ell \cdot |x|}{D^2} + \theta \right\} + \dots \\
 & \dots + \frac{1}{4(4!)} \left(\frac{D}{p} \right)^4 \left\{ \frac{\ell^3 \cdot |x|}{D^4} + \frac{3}{2} \left[\frac{\ell \cdot |x|}{D^2} + \theta \right] \right\} + \dots \\
 & \dots + \frac{1}{6(6!)} \left(\frac{D}{p} \right)^6 \left\{ \frac{\ell^5 \cdot |x|}{D^6} + \frac{5}{3} \left[\frac{\ell^3 \cdot |x|}{D^4} + \frac{3}{2} \left[\frac{\ell \cdot |x|}{D^2} + \theta \right] \right] \right\} + \dots \\
 & \dots + \frac{1}{8(8!)} \left(\frac{D}{p} \right)^8 \left\{ \frac{\ell^7 \cdot |x|}{D^8} + \frac{7}{4} \left[\frac{\ell^5 \cdot |x|}{D^6} + \frac{5}{3} \left[\frac{\ell^3 \cdot |x|}{D^4} + \frac{3}{2} \left[\frac{\ell \cdot |x|}{D^2} + \theta \right] \right] \right] \right\} + \dots \tag{8}
 \end{aligned}$$

Fourth term S_4

$$\begin{aligned}
 S_4 = & + \left\{ \frac{1}{1(1!)} \left(\frac{D}{p} \right) \left\{ \left(\frac{|x|}{D} \right) + \dots \right. \right. \\
 & \dots + \frac{1}{3(3!)} \left(\frac{D}{p} \right)^3 \left\{ \frac{\ell^2 \cdot |x|}{D^3} + \frac{2}{1} \left(\frac{|x|}{D} \right) \right\} + \dots \\
 & \dots + \frac{1}{5(5!)} \left(\frac{D}{p} \right)^5 \left\{ \frac{\ell^4 \cdot |x|}{D^5} + \frac{4}{3} \left[\frac{\ell^2 \cdot |x|}{D^3} + \frac{2}{1} \left(\frac{|x|}{D} \right) \right] \right\} + \dots \\
 & \dots + \frac{1}{7(7!)} \left(\frac{D}{p} \right)^7 \left\{ \frac{\ell^6 \cdot |x|}{D^7} + \frac{6}{5} \left[\frac{\ell^4 \cdot |x|}{D^5} + \frac{4}{3} \left[\frac{\ell^2 \cdot |x|}{D^3} + \frac{2}{1} \left(\frac{|x|}{D} \right) \right] \right] \right\} + \dots \\
 & \dots + \frac{1}{9(9!)} \left(\frac{D}{p} \right)^9 \left\{ \frac{\ell^8 \cdot |x|}{D^9} + \frac{8}{7} \left[\frac{\ell^6 \cdot |x|}{D^7} + \frac{6}{5} \left[\frac{\ell^4 \cdot |x|}{D^5} + \frac{4}{3} \left[\frac{\ell^2 \cdot |x|}{D^3} + \frac{2}{1} \left(\frac{|x|}{D} \right) \right] \right] \right] \right\} + \dots \tag{9}
 \end{aligned}$$

It is noted that the aforementioned leading terms are frequency dependent whilst the nested terms depend only on the geometry of the cable system.

A. Series and numerical integration

Consider the three cable application case reported in [1] which is also reproduced here below in Fig. 2. For this case, the frequency range has been uniformly sampled testing from 1Hz to 10MHz by using 100 equidistant points.

As a first evaluation step, we use the series proposed by Wedepohl-Wilcox, S_{ser} , given by (5). The second evaluation corresponds to the trapezoidal numerical integration (a step equal to 10^{-4} is used) of the third right-hand-side integral expression in (4c), labeled as S_{int} .

The behavior of both evaluations is presented in Fig. 3a. In this figure, the real and complex components of S_{int} are presented in black continuous dotted line. As for S_{ser} , the number of terms has been varied and the corresponding result is shown in gray dashed line.

From the results shown in Fig. 3a, it can be noticed that the first four terms of each S_n , $n = 1, \dots, 4$, give a fairly good agreement compared to S_{int} . Further evaluations including more than four terms did not produce important differences between evaluation methods for S_{ser} . This corresponds to the theory of convergence of a series around a given point [6].

B. Ratio test

In addition, the uniform convergence of the sequence of partial sums (or series solution S_n) has been calculated by using the following ratio test [3], for $n = 1, 2, 3$, and 4:

$$\lim_{k \rightarrow \infty} \left| \frac{S_{n_{k+1}}}{S_{n_k}} \right| < 1 \tag{10}$$

The results of evaluating (10) are shown in Fig. 3b. From this numerical analysis, one can observe the smooth behavior of the four set of curves S_n when approximating to S_{ser} , thus indicating a uniform convergence feature, as defined in [6].

C. Alternative series-based solution

As presented in [3] and here in Fig. 3, it can be seen that all four terms of the series give accurate results, at very low computational expenses, up to $D/|p| \approx 2$. Therefore, it was proposed in [3] to use this ratio as a limit criterion to generate a hybrid algorithm that switches between series and any simple numerical integration routine.

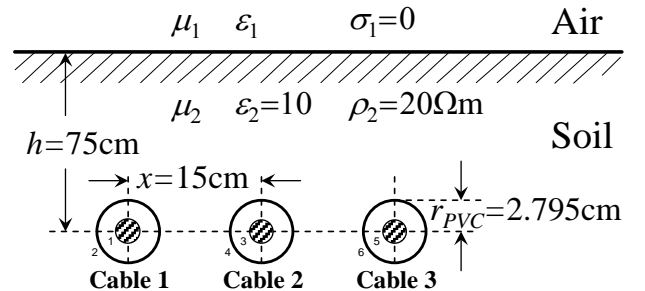


Fig. 2. Underground cable transmission system, taken from [1].

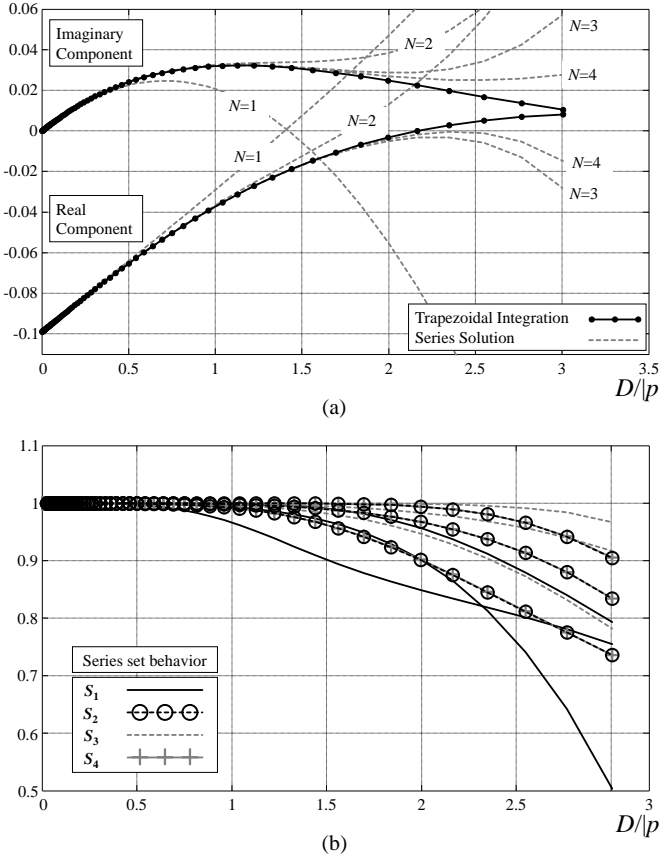


Fig. 3. Series convergence test. (a) Comparison between series solution and hybrid technique regarding the number of terms. (b) Ratio test

Notice that this condition contrasts with the one proposed in [1] where $D/|p| = 1/4$ is used to switch between the series solution and the closed form solution of (2) obtained from the leading terms of the same series expansion developed in (5).

Furthermore, an important aspect in the proposed hybrid algorithm in [3], is the inclusion of the displacement currents in the ground, as indicated in (1b).

The here presented results have been obtained for the particular case of analyzing the underground cable system configuration proposed in [1] which is shown in this paper in Fig. 2. However, a similar analysis can be directly extended to a broad range of real cable configurations.

D. Hybrid technique

In the here proposed technique to calculate Z_g the simple analytical functions from (2), (3a) and (4) are combined with the numerical integration of S_{int} as shown below:

$$Z_g(\omega) = \frac{j\omega\mu_0}{2\pi} \left[K_0(d/p) - K_0(D/p) + \frac{2\ell^2}{D^2} K_0(D/p) + \dots \right. \\ \left. \dots + \frac{2p[\ell^2 - x^2]}{D^3} K_1(D/p) - \frac{2p^2[\ell^2 - x^2]}{D^4} \left(1 + \frac{\ell}{p} \right) \cdot e^{-\frac{\ell}{p}} \dots \right. \\ \left. \dots - \frac{2x\ell}{D^2} S_{int} \right] \quad (11)$$

where, as described in section III. A:

$$S_{int} = \int \frac{1}{D} \left[2\sqrt{1-t^2} - \frac{1}{\sqrt{1-t^2}} \right] \cdot e^{-\frac{D}{p}t} dt \quad (12)$$

As shown in Fig. 3a, it is evidenced that the behavior of S_{ser} and S_{int} are very similar for values $D/|p| \approx 2$. From this point of view a new methodology based on the mathematical properties of S_{int} can be proposed regarding the improvement of accuracy and CPU-time.

As an illustrative example, the integrand behavior of (12) is shown in Fig. 4 taking 100 regular samples of frequency from 1Hz to 10MHz, for the cable system in Fig. 2.

The numerical integration of (12) is shown in Fig. 5. This solution has been obtained testing three different types of quadrature routines: Gauss-Kronrod quadrature, Romberg Mid-pint-rule and Trapezoidal integration.

As it can be seen from Fig. 4 and Fig. 5, the asymptotic oscillatory behavior of the integrand of (12) strongly depends on the physical and media parameters of the cable system.

After testing several cases of different cable systems solving (12) with the aforementioned numerical integration routines, an optimal calibrated trapezoidal solution is obtained. In the sense of a fast and accurate enough for this paper application cases.

Thus, for simplicity the trapezoidal numerical solution of S_{int} is chosen to complement the calculation of Z_g in (11) which is the here proposed technique taken as a reference which performance and accuracy are tested in the following paper section.

IV. MUTUAL GROUND-RETURN IMPEDANCES COMPUTATIONAL ANALYSIS

In this section the computational performance of the: 1) Hybrid technique solving (11), 2) Wedepohl *et al.*, series (4d), 3) Direct Pollaczek integral evaluation through Gauss-Kronrod in (2) and 4) Images based formula (SGG) from [4] for calculating mutual Z_g for the underground cable system shown in Fig. 2 is analyzed here regarding rms-error and CPU-time.

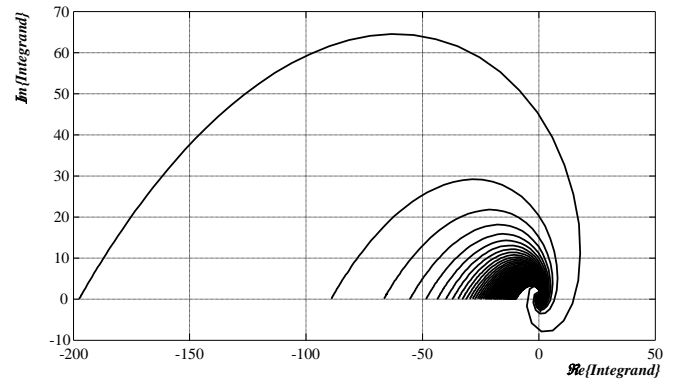


Fig. 4. Phase plane for the integrand behavior for the cable system shown in Fig. 2 sampled for a vector frequency of $1\text{Hz} \leq f \leq 10\text{MHz}$.

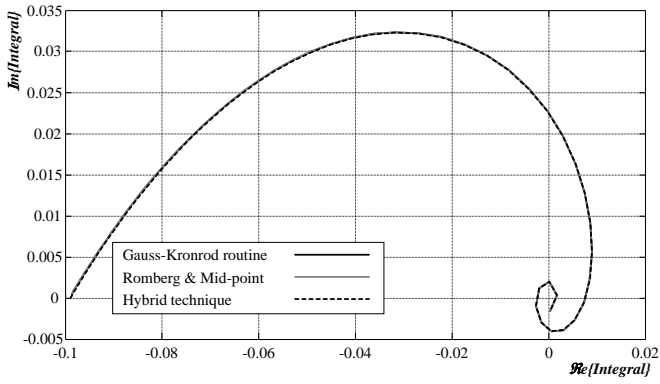


Fig. 5. Numerical solution of (12) for the cable system in Fig.2 using three different generic quadrature routines.

This test is performed for calculating mutual Z_g varying the horizontal distance “ x ”, between two buried cables (see Fig. 1), according to $0.001\text{m} \leq x \leq 2\text{km}$.

The ground resistances are shown in Fig. 6a testing three frequencies, while in Fig. 6b the mutual ground inductances are also depicted.

It can be seen from these two figures that the curves behavior calculated with the aforementioned methods are in good agreement with the here proposed hybrid technique (taken here as a reference solution and also in Table I).

On one hand, for a quantitative evaluation, the relative errors ($\% \varepsilon_{rel}$) for each of the three frequency curves between the hybrid technique solving (11) and the other three approximate techniques are shown in Fig. 7, through the following expression:

$$\% \varepsilon_{rel} = \left| 1 - \frac{f_{approx}}{f_{exact}} \right| \times 100 \quad (13)$$

where f_{approx} and f_{exact} , mean the corresponding approximated and exact function evaluations, respectively.

In this numerical experiment, the series solution of [1] implemented in [3], has presented small discontinuities at the bottom of Fig. 7. As in the case of Carson’s series [3] and [5] this is due in part to the switch between low and high frequency boundary series.

The Gauss-Kronrod quadrature routine presented small numerical oscillations at the final stage of the figure. The presence of this type of discontinuities is the evidence that the integrand may have a singularity at one of the integration limits.

The SGG formula presented a relative error as much as 24% for the three frequency tested curves at certain distances, only. However, SGG formula was based in the method of images taken the ground plane as a mirror, which means that the closer the cable conductors, the accurate the calculation of Z_g .

On the other hand, for a qualitative evaluation, Table I resumes the obtained rms-error and the computational CPU-time required for calculating Z_g for each frequency curve with the four tested methods.

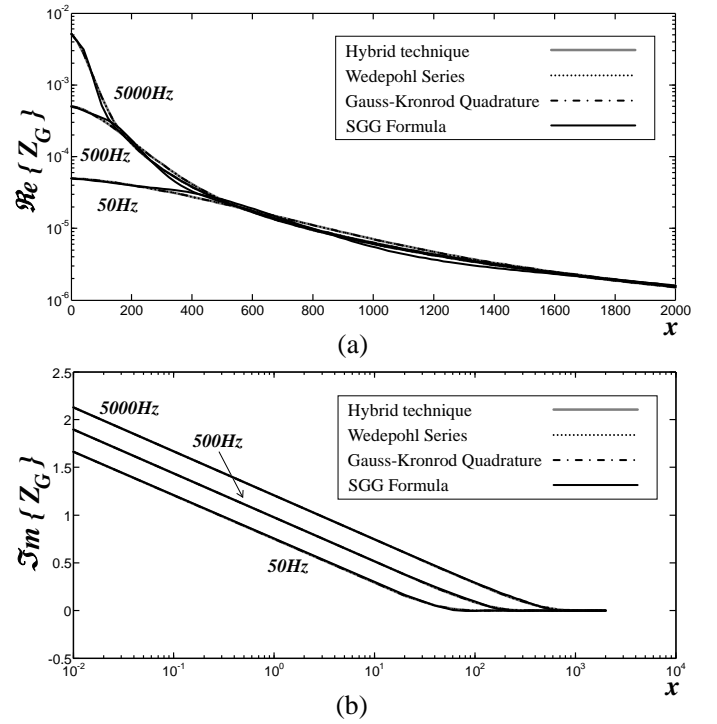


Fig. 6. Mutual ground impedances calculated solving (12) with hybrid technique and applying for comparison Wedepohl series, Gauss-Kronrod routine and SGG Formula. a) Resistances. b) Inductances

In electromagnetic transients calculation [5], the required accuracy and CPU-time are very important variables, even more when certain line or cable models can be considered for further real-time applications [7].

The numerical results shown in Table I were obtained using Matlab® v7.8 on a 2.4GHz processor with 4GHz of RAM.

From Table I can be observed that the computational time required by the Gauss-Kronrod method is larger than any other of the compared methods, as expected.

The Wedepohl *et al.*, series solution also takes more CPU time compared to the hybrid technique proposed here; also, the rms-error increases for larger values of frequency.

This is perhaps due to the criterion for switching between the series and the closed-form formula in [1].

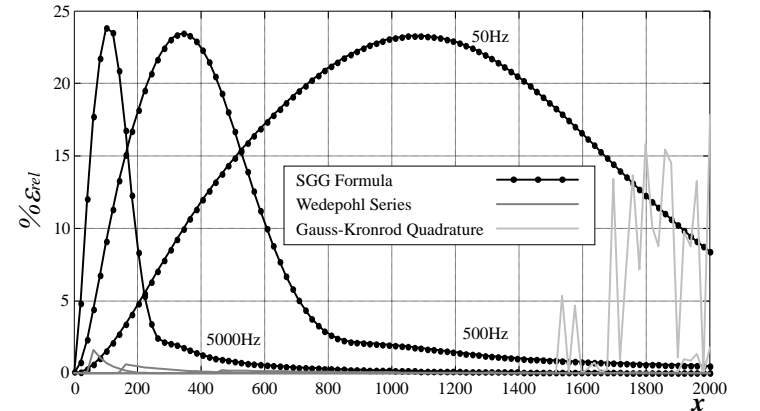


Fig. 7. Relative errors between the proposed method in comparison with SGG formula, Wedepohl series and the Gauss-Kronrod quadrature routine.

The SGG formula presented a very similar CPU-time than the proposed hybrid technique for the last frequency case. However, its rms-error is the largest one between any of the here treated approximate solutions, but this is indicating that probably this formula was not developed for large horizontal distances between underground cables bigger than usual engineering practical installations. In many other cases, this formula has proven to be very accurate [4].

TABLE I
RMS ERROR AND CPU TIME

		Test Methodology			
		Hybrid technique	Gauss-Kronrod	Wedepohl Series	SGG Formula
50Hz	CPU time (Sec)	0.0312	2.1840	0.1404	0.0156
	rms error	(base)	0.0006e-3	0.1930e-3	0.0247
500Hz	CPU time (Sec)	0.0468	1.8720	0.0312	0.0156
	rms error	(base)	0.0117e-3	0.3913e-3	0.0186
5KHz	CPU time (Sec)	0.0156	1.4508	0.0468	0.0156
	rms error	(base)	0.1163e-3	0.6558e-3	0.0127

V. CONCLUSIONS

The Wedepohl *et al.*, series formulation to calculate ground-return impedances of underground power cables has been implemented and the numerical results are analyzed in this paper.

This series solution is highly efficient and converges rapidly at the low-frequency range. However, when combined with the closed-form solution taken from the only leading terms of the series as indicated in [1], lacks precision in the range of about 1×10^{-3} rms.

There are some other techniques for the direct numerical integration of Pollaczek's using automatic or adaptive quadrature routines as the Gauss-Kronrod technique.

In the here presented application case the Gauss-Kronrod technique results to be accurate for almost the entire frequency range. However, it requires a long CPU-processing time and at certain ranges this quadrature routine has produced numerical discontinuities.

It has been already reported in the literature that the SGG formula is accurate enough for many practical engineering applications. In this paper the horizontal distance between cables has been set to 2km, which is probably out of the application range of this image based formula. However, this validity range has not been reported yet in the specialized literature.

Thus, a new hybrid technique for calculating Z_g (partly

analytical-numerical) is proposed and its performance is analyzed here. The obtained results yields that this method is accurate enough that can be compared with the direct solution of the Pollaczek integral and its required processing time is short as in the case of solving an analytical formula.

Finally, this method can be used to define practical application ranges for other approximate formulas and also to assess other numerical methods (as the ones based on quadrature, infinite series, conformal mapping, numerical optimization, etc.) for improving accuracy on transient calculations.

VI. APPENDIX

Cable layout for the transient case reported in [1] and also depicted in Fig. 2.

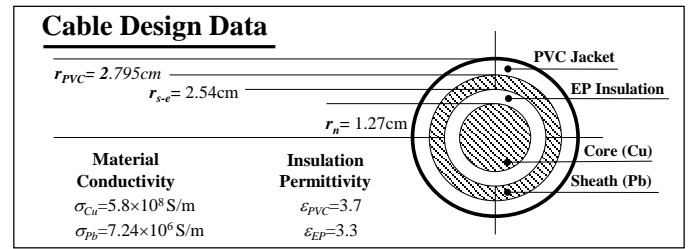


Fig. 8. Original cable layout for the cable system taken from [1].

VII. REFERENCES

- [1] L. M. Wedepohl and D. J. Wilcox, "Transient analysis of underground power-transmission systems", Proc. IEE, vol. 120, No. 2, pp. 253-260, February 1973.
- [2] F. Pollaczek, "Über das Feld einer unendlich langen wechselstromdurchflossenen Einfachleitung", Electriche Nachrichten Technik, Vol. 3, No. 9, pp. 339-360, 1926.
- [3] F. A. Uribe and A. Ramirez, "Alternative Series-Based to Approximate Pollaczek's Integral", IEEE Trans. on Power Delivery, Vol. 27, No. 4, October 2012, pp. 2425-2427.
- [4] O. Saad, G. Gaba and M. Giroux, "A closed-form approximation for ground return impedance of underground cables", IEEE Trans. on Power Delivery, vol.11, No.3, pp. 1536-1545, July 1996.
- [5] W. Dommel, Electromagnetic Transients Program Reference Manual (EMTP Theory Book), Prepared for Bonneville Power Administration, P.O. Box 3621, Portland, Ore., 97208, USA, 1986.
- [6] W. Kaplan, Advanced Mathematics for Engineers. Addison Wesley, 1981.
- [7] T. Noda, "Numerical techniques for accurate evaluation of overhead line and underground cable constants," IEEJ Trans., Electrical and Electronic Engineering, vol. 3, Issue 5, pp. 549-559, 2008.